GROUND PENETRATING RADAR FOR GEOTECHNICAL APPLICATIONS

Jeffrey J. Daniels ***Roger L. Roberts***

The Ohio State University
Department of Geological Sciences
Columbus, Ohio 43210, USA

SYNOPSIS : Ground penetrating radar (GPR) is a relatively new technique for investigating a broad spectrum of applications to detect and define shallow geologic, engineering and hydrologic features. It is the only geophysical technique currently in use that can provide a high resolution picture of the shallow subsurface in a manner similar to the seismic technique which is used for deeper geologic targets. In addition to normal geophysical interpretive skills, proper interpretation of GPR measurements requires an understanding of antennas, and the propagation of electromagnetic waves through the shallow subsurface.

The primary objectives of this paper are to: (1) provide information on the principles of GPR measurements, and (2) demonstrate the use of these measurements to solve problems in mining, geotechnical engineering, and hydrogeology. It is hoped that this paper will contribute to bridging the gap between agronomists, engineers, geologists, hydrogeologists, geophysicists, and others by contributing to a common basis for a better understanding of the subject.

INTRODUCTION

Geophysical techniques measure the physical properties of the subsurface, with the measurement instrumentation placed above the surface. Summaries of the fundamentals of geophysical techniques for hazardous waste site evaluation have been given by Ulriksen (1982), Benson, and others (1984), and Daniels (1989). The overriding objective of site specific geophysical investigations is to provide in-situ evaluation of subsurface conditions and processes without drilling or excavation. Geophysical techniques have the ability to measure the same physical and chemical properties over a wide range of scales (from centimeters- to- kilometers) and provide a link between the different modeling scales used by hydrogeologists and engineers.

The only proven non-invasive geophysical techniques that have the potential of providing detailed images of the subsurface are: 1) acoustic techniques, and 2) ground penetrating radar (GPR). Unfortunately, neither of these methods has been developed to their full potential for geotechnical applications. The acoustic techniques that have been developed require laborious, manpower intensive, field procedures. Acoustic techniques have a great potential, but the prevailing thinking and procedures that have worked for the petroleum industry will need to be changed before acoustic techniques can be applied to complex situations encountered in engineering applications. This paper presents an overview of the basic principles of the hardware, software, and field application procedures for the ground penetrating radar technique.

OPERATING PRINCIPLES

Overview

GPR has been developed over the past thirty years for shallow, high resolution investigations of the subsurface. The present modus-operandi for GPR produces a two dimensional cross section (sometimes called a record) of the subsurface that is similar in appearance and interpretation to a seismic cross section. Field operation of a GPR system is very simple and data can be acquired very rapidly. Presently, it is not uncommon to tow the antennas behind an All Terrain Vehicle (ATV) and collect several line-kilometers of data along profile lines spaced a few meters (or fractions of meters) apart. These high data densities ultimately can be exploited to produce three dimensional images of the subsurface. The mobility and simple field procedures inherent to GPR make it a natural technique for geotechnical applications.

GPR uses the principle of the reflection of electromagnetic waves to locate buried objects. The basic principles and theory of operation for GPR are the same as those used to detect aircraft overhead, but GPR uses a much broader bandwidth, and transmitting and receiving antennas that are pointing downward into the ground (see Figure 1).

A transmitting antenna launches an electromagnetic wave (25 Mhz to 1 Ghz) into the ground (Figure 1a). The wave spreads out and travels downward until it hits an object that has different electrical properties from the surrounding ground. The surface surrounding the advancing wave is called a wavefront. A straight line drawn from the transmitter to the edge of the wavefront is called a ray. Rays are used to show the direction of travel of the wavefront in any direction away from the transmitting antenna. If the wave hits a buried object, then part of the wave's energy is "reflected" back to the surface (Figure 1b), while part of its energy continues to travel downward. The wave that is reflected back to the surface is captured and recorded on a digital storage device for later interpretation.

In practice, GPR measurements are made by towing the antennas continuously over the ground. The antennas can be towed by pulling them by hand, or with a vehicle (usually an ATV). A radar wave is transmitted and received each time that the antenna has been moved a fixed distance across the ground surface. Usually, this distance (called the trace spacing) is less than 0.3 m. Every time that the antennas have traveled a distance equal to the trace spacing, the following sequence of events occur in the GPR system: 1) a wave is transmitted, 2) the receiver is turned on to "wait" to receive reflected signals, and 3) after a certain period of time (usually less than one microsecond) the receiver is turned off. The information that is recorded while the receiver is turned on is called a trace. A trace contains the reflections that have bounced back from the buried objects below the receiver (see attached Figure 2). A reflection is detected on a trace from the increase in the signal amplitude that occurs at a certain time after the receiver is turned-on. It takes a specific amount of time for the electromagnetic wave to make the round-trip from the surface down to the reflector, and back to the surface. Travel times for electromagnetic waves

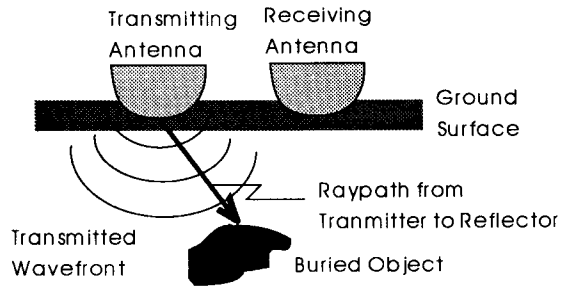

(a) Radar wave transmitted as a cylindrical spreading wave.

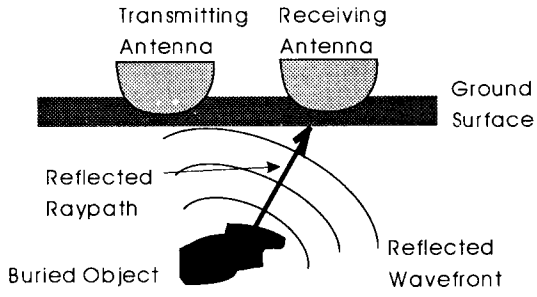

(b) Reflected wave from a point on a buried object.

Fig. 1. The GPR reflection process.

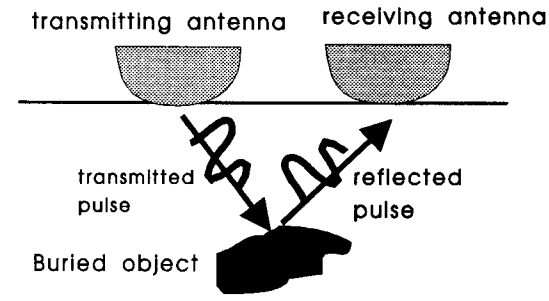

(a) An electromagnetic pulse is transmitted, travels through the ground, is reflected, and travels to the receiver antenna.

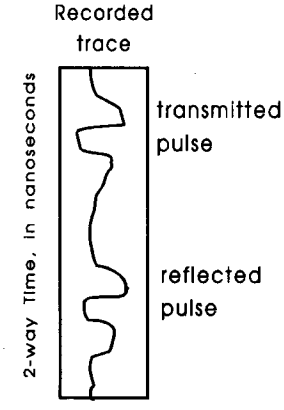

(b) A simple trace from a buried object consists of the transmitted pulse traveling through the air and the reflected pulse.

Fig. 2. The making of a single time trace, with transmitter and receiver antennas at a single point on the surface.

are measured in nanoseconds (1 nanosecond = 10^{-9} seconds). The abbreviation for nanosecond is "ns". The travel time for an electromagnetic wave in air is approximately 3.3 ns per m traveled. The round-trip (or two-way) travel time is greater for deep objects than for shallow objects. Therefore, the time of arrival for the reflected wave recorded on each trace can be used to determine the depth of the buried object, if the velocity of the wave in the subsurface is known.

A single trace can be used to detect objects (and determine their depth) below a spot on the surface. By towing the antenna over the surface and recording traces at a fixed spacing, a record section of traces can be constructed (see Figure 3). The horizontal axis of the record section is surface position, and the vertical axis is round-trip travel time of the electromagnetic wave. A GPR record is very similar to the display for an acoustic sonogram, or the display for a fish finder. Two types of recordings of GPR traces are shown in Figure 4, including: a) a wiggle trace display, where the intensity of the received wave at an instant of time is proportional to the amplitude of the wiggle, and b) a gray-scale display, where the intensity of the received wave at an instant in time is proportional to the intensity of gray scale (i.e. black is high intensity, white is low intensity). The process of converting a wiggle trace to a gray scale (or color) scan is illustrated in Figure 5.

When the traces are displayed as a cross section, the size, shape and depth of objects can be determined. The depth to the top of the object is computed by dividing the two-way travel time to the object by two times the velocity of the electromagnetic wave through the ground:

$$Depth = \frac{2\ way\ travel\ time}{2x(velocity\ of\ the\ wave)} \qquad (1)$$

Typical ranges for two-way travel-time range settings are 10-to-500 ns. The velocity (or speed) of the radar wave is expressed in units of distance/time, where distance is expressed either in feet, or meters, and time is expressed in nanoseconds. The velocity of the electromagnetic wave depends primarily upon the relative permittivity (sometimes called the dielectric constant, or dielectric permittivity) of the rock, soil, or other material. The relative permittivity is the ratio of the permittivity of the material divided by the permittivity of air, or:

$$\epsilon_{rm} = \frac{\epsilon_m}{\epsilon_o} \qquad (2)$$

The range for relative permittivity values is from 1 (for air) to 81 (for water). In general, the velocity of a radar wave in a material can be calculated from

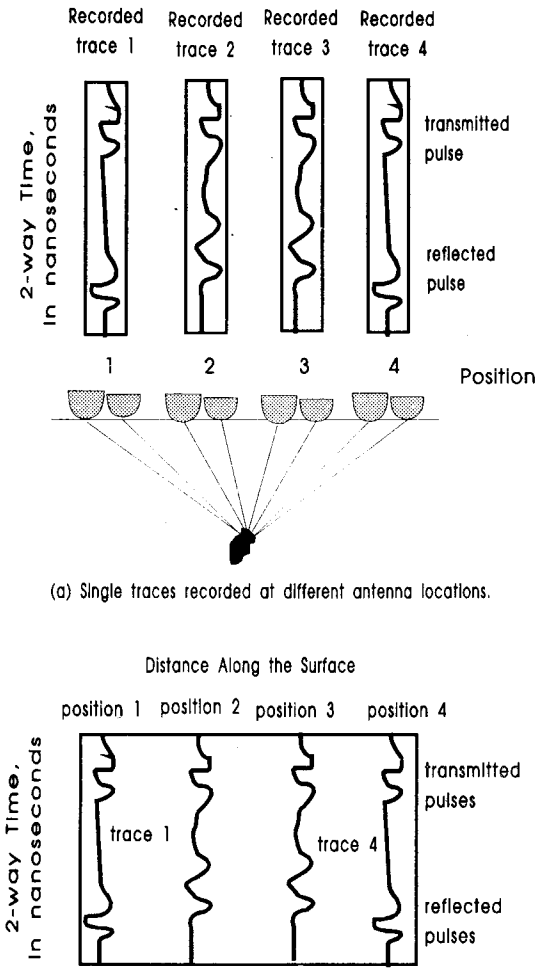

Fig. 3. The process of combining traces, recorded at even spacings on the surface, to form a GPR record.

the following relationship:

$$Velocity = \frac{Velocity\ of\ a\ radar\ wave\ through\ air}{\sqrt{relative\ permittivity\ of\ the\ material}} \quad (3)$$

The velocity of a radar wave in air is approximately 1 ft/ns in English length units (0.305 m/ns in metric units). The velocity of a radar wave in water (relative electric permittivity = 81) is equal to 0.0339 m/ns. The relative permittivity of a clean sand, or homogenous granite, is approximately equal to 5, with a velocity of approximately 0.13625 m/ns.

In order to interpret the data more accurately, the electrical characteristics of the media are measured at various depths on the day of the experiment. Electrical properties can be measured by inserting a capacitive probe developed by Caldecott et al. (1985) into a shallow auger hole. The probe operates at 40 Mhz and it is assumed the properties of the media vary slowly with frequency so they can be used to approximate the entire range of consideration. Usually one borehole is used to approximate the test area and measurements are taken at 10 cm depth increments.

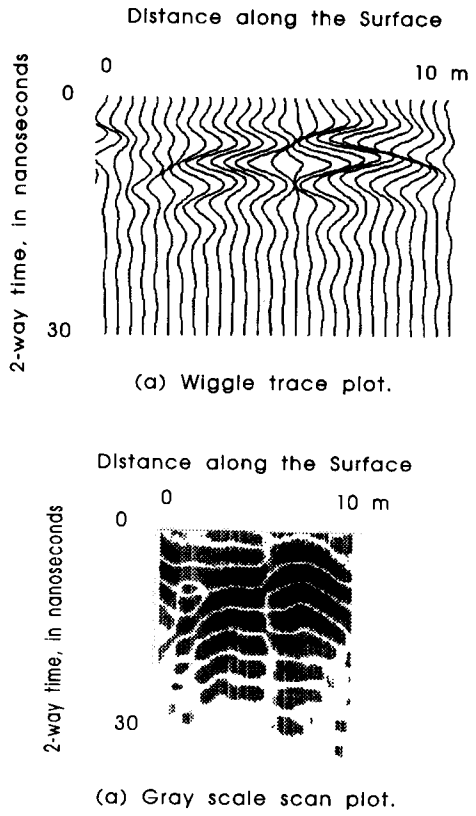

Fig. 4. Comparison of wiggle trace and gray scale scan record displays. Anomalies are caused by two buried barrels.

Reflections are caused by an abrupt change in the velocity, or conductivity, of the material in the subsurface. Some common features that have a high velocity contrast include: 1) empty cavities, voids, or tunnels, 2) changes in rock porosity, 3) the water table, 4) plastic containers, 5) concrete foundations, 6) oil, petroleum, DNAPL spills, or 7) changes in geology. Conductive features in the subsurface include barrels, tanks, pipes, clay, and salts dissolved in the groundwater.

Reflections from objects that appear on the GPR record are often referred to as anomalies. The location, size, and shape of anomalous features on the record are a function of the depth, size and shape of the buried objects. Objects in the subsurface causing anomalies on a single GPR record can be classified as either one dimensional, two dimensional, or three dimensional. Figure 6 depicts the shape of the anomalies caused by one and two dimensional buried objects. A one dimensional anomaly is caused by a horizontal planer interface (e.g. earth strata, a water table, etc.), which will show up on the GPR cross section as a flat anomaly (see Figure 6a). However, all anomalies from objects with distinct edges are curved, and objects with edges (or curvature) are considered two dimensional. A two dimensional anomaly can be caused by crossing a non-planer, non-horizontal, object (e.g. a dipping fault plane, buried pipe, etc.). An anomaly that has a parabolic shape is indicative of a two dimensional object (e.g. a dipping fault plane, a buried pipe, etc.), when interpreted from a single GPR record.

This can be seen from the anomaly over the barrels in Figure 6b. The parabolic anomaly can be understood from the fact that the radar wave from the transmitter spreads out in front of -, under-, and behind the antennas.

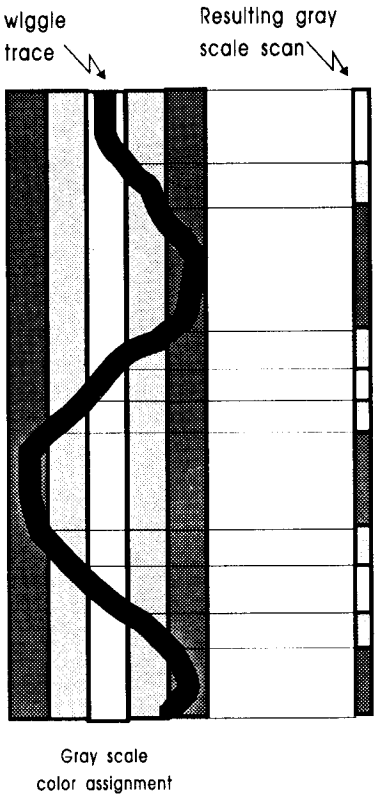

Fig. 5. Gray scale (or color) assignment procedures. Gray shades are assigned to different amplitudes on the wiggle trace, producing a gray scale scan.

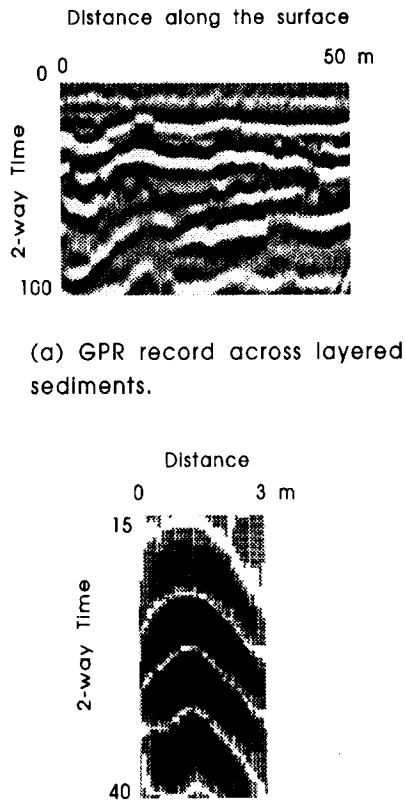

Fig. 6. Example of GPR scan records over (a) layered sediments, and (b) a buried barrel.

Therefore, reflections are received from an object: 1) prior to crossing over the object, 2) when the antennas are over the center of the object, and 3) when the antennas are moving away from the object. Since the distance is increasing as the antennas are moved away from the object, the two-way travel time increases, causing the parabolic shape of the anomaly on the GPR record. Fishermen can observe the same curved "anomalies" on the displays for acoustic fish-finders when the boat passes over a fish.

GPR Systems And System-Target Interaction

The transmitter and receiver of a GPR system may either be separate (Figure 1), or the same antenna may be utilized to transmit and receive the signal. A system with a separate transmitter and receiver is called bistatic, while a system utilizing the same antenna for the transmitter and receiver is called a monostatic system. In either case, the transmitter sends out an electromagnetic wave as the source signal. Theoretically, this is a pure, consistent, signal that is independent of variations caused by the electronics, or the electrical properties of the ground. All antennas are designed to perform optimally under certain conditions (including specific electrical properties of the ground), and the system will not operate as designed when these conditions are not met. Another important practical feature of antennas is shielding, which determines the amount of interference that is received from objects above the ground surface. High frequency antennas are usually shielded by placing material above the antennas that absorb electromagnetic radiation. Low frequency antennas (< 200 Mhz) are rarely shielded, since it is very difficult to absorb long wavelength signals.

Most GPR systems use a time-domain pulse system (Miller, 1986), and nearly all of the systems that are used for engineering and environmental applications (including Geo-Centers, GSSI, and Sensors and Software) utilize a time-domain pulse system. The primary advantage of pulse systems is that records from the pulse source can be interpreted directly from the receiver without any pre-processing. The antenna is often identified by its approximate center-band frequency (eg. 80Mhz, 100 Mhz, etc.). In general, a high frequency antenna has a higher resolution and a lower depth penetration (higher attenuation) than a low frequency antenna.

Most GPR antennas manufactured commercially are elongate in one dimension, and when the antenna is excited by a voltage impulse, the currents are directed along the long axis of the antennas. Consequently, radiation emitted from these antennas is polarized parallel to their long axis, and the behavior of these GPR antennas is similar to dipole antennas. Elongate, dipole-like, GPR antennas do not radiate equally in all directions. When a dipole antenna is placed horizontally near the ground, most of the radiated energy penetrates into the ground. In the ground, the energy distribution can be approximated as an elliptically shaped beam, as shown in Figure 7. The long axis of the ellipse is perpendicular to the long axis of the antenna. It is clear that the orientation of the antenna relative to the buried target influences the amount of electromagnetic energy impinging on a buried target.

As the polarized waves propagate through the subsurface, they reflect and diffract from objects with electrical properties different from the host

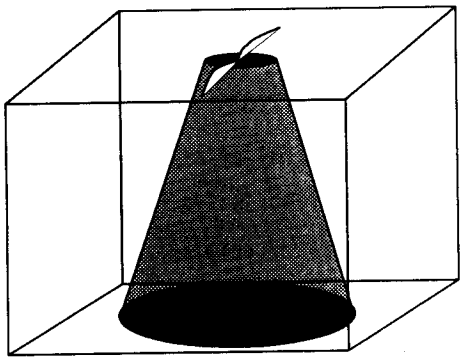

Fig. 7. Field pattern of antenna is elongate transverse to the long axis of the antenna.

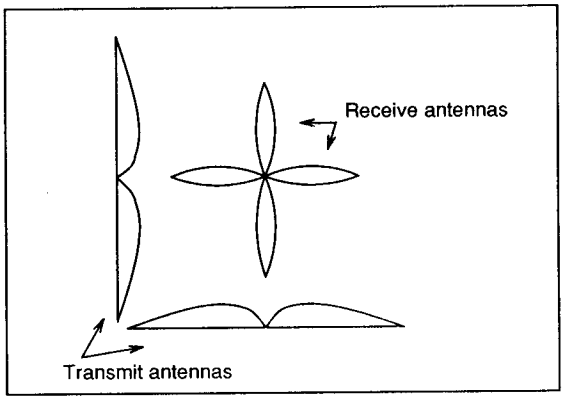

Fig. 8. Antenna setup used to collect multiple polarization GPR data.

medium. The amplitude of the reflection energy measured by the receiver antenna is dependent on a number of different factors including: target distance from the transmitting and receiving antennas; target composition; target geometry; target orientation with respect to the transmitting antenna; and the electrical properties of the host medium.

Generally, the ground can be considered a lossy medium, where electromagnetic waves propagating through the ground are exponentially attenuated. The electrical properties of the ground and the distance of the buried target from the transmit and receive antennas determines the amount of wave attenuation during propagation. If the buried target is an interface between two horizontal layers, then the contrast in electrical properties between the two media determines the strength of the reflection from the interface. However, if the buried target has finite dimensions in two, or three, directions (e.g. a barrel or a pipe), then the shape and dimensions of the target also influence the reflected energy strength. In addition, if the propagating electromagnetic waves are radiated from an elongate GPR antenna, they are polarized, and the angle of the polarization with respect to the target orientation may have a significant influence on the reflected energy.

Research at The Ohio State University has been conducted on analyzing the importance of antenna field pattern and polarization related to GPR investigations (Roberts and other, 1993). A two-channel GPR control unit and multiple antenna set-up have been developed during the course of the research. GPR data are acquired using the equipment over targets buried in a GPR test pit 4.9 m x 5.5 m x 2.6 m in dimensions and filled with clean, washed sand.

The multiple antenna set-up is shown in Figure 8. The two outer antennas serve as transmitters. A switch is used to excite one antenna, then excite the other antenna. The two inner antennas are commonly called "crossed-dipole" antennas. These antennas are dedicated receivers. During data collection, one outer antenna transmits, and the energy reflected from subsurface targets is received at the two inner antennas. One of the inner antennas is parallel to the transmit antenna. The energy collected at the parallel receive antenna has the same-sense polarization as the transmitted waves. Energy received at the other inner antenna is termed "cross polarized" energy. The strength of this return relative to the parallel polarized energy depends on the target geometry and orientation relative to the transmit antenna.

The field pattern of GPR antennas can be measured by burying a sphere and collecting GPR data over the sphere in a two dimensional grid. A sphere is a desirable target because its reflection coefficient is independent of the incident wave's polarization. Figure 9 shows GPR data collected in the test pit over and offset from a 0.5 m diameter metallic sphere buried 0.5 m. Profile line H was offset horizontally less than one meter from the sphere, yet the sphere's reflection is barely discernible in the data. These data show that most of the antenna's radiated power is directed vertically downward.

Figure 10 shows the ellipticity in the field pattern for antennas oriented parallel to the profile line direction and transverse to the profile line over a 0.5 m diameter metallic sphere buried at 0.25, 0.5, 0.75 and 1.0 m depths. Comparison of the GPR records over the sphere buried 0.25 m shows strong reflections over, and offset from, the sphere in the data set collected with transmit and receive antennas oriented transverse to the profile line. While the measurements from antennas oriented parallel to the profile line show a strong reflection over the sphere, but very weak arrivals immediately offset from the sphere. This is a direct result of the ellipticity in the field pattern. Data from the sphere buried at increasing depths reveal that the asymmetry in the field pattern tends to decrease. A comparison of the profile line data over the sphere buried 1.0 meters shows a similarity between data measured with antennas transverse and parallel to the profile line direction. Therefore, the ellipticity in the field pattern is most pronounced very near the antenna.

The reflection strength from a target is independent of the polarization of the impinging waves for targets that have three dimensional symmetry and a smooth surface. However, if the target is asymmetrical, or only has two-dimensional symmetry (e.g. barrels), then the reflection strength from the target may be strongly dependent on the orientation of the target relative to the transmitting antenna. Buried pipes are extremely sensitive to wave polarization. Metallic pipes are strong reflectors if the long axis of the transmitting antenna is parallel to the pipe axis. The reflection strength from the pipe decreases proportional to the sine of the angle made by the pipe and the transmitting antenna axis (Daniels and others, 1988). The profile lines in the top row of Figure 11 are parallel polarized measurements along profile lines that are oriented at different azimuths relative to the long axis of a pipe buried 0.5 m in the GPR test pit. The reflection strength decreases to the point where it is indistinguishable from background noise at a 15 degree angle.

The fact that some targets are very sensitive to electromagnetic wave polarization can be exploited, since these targets cause a phenomenon called depolarization when they are not oriented symmetrically with respect to the transmit antenna. Part of the loss in parallel polarized reflection strength is from waves reflecting off the target at a different polarization than the impinging waves. The antenna in the center of the setup in Figure 8 is sensitive to depolarized waves reflected back towards it when using the outer antenna perpendicular to it as a transmitter.

The second row of data in Figure 11 shows cross-polarized reflections from profile lines crossing over the buried pipe at different azimuths. Note, significant cross-polarized energy is observed along profile lines not oriented

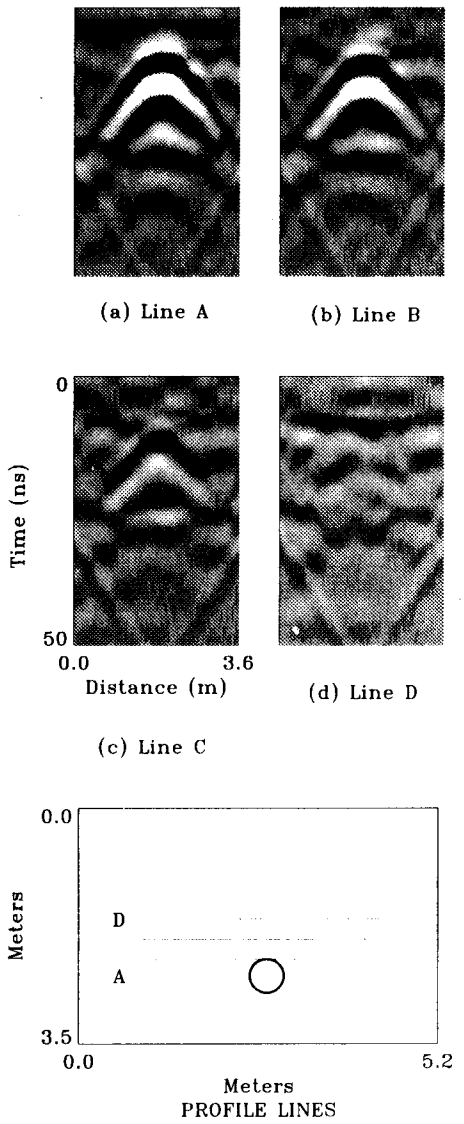

Fig. 9. Profile line data at increasing offset distances from a 0.5 m diameter metal sphere buried at a depth of 0.5 m. (from Roberts and others, 1993)

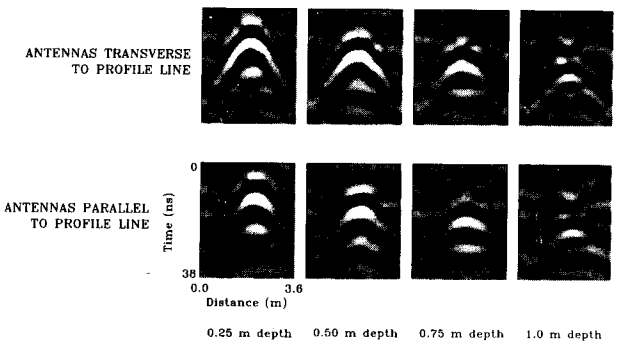

Fig. 10. Profile lines with different antenna orientations crossing over sphere buried at depths of 0.25, 0.50, 0.75, and 1.0 m.

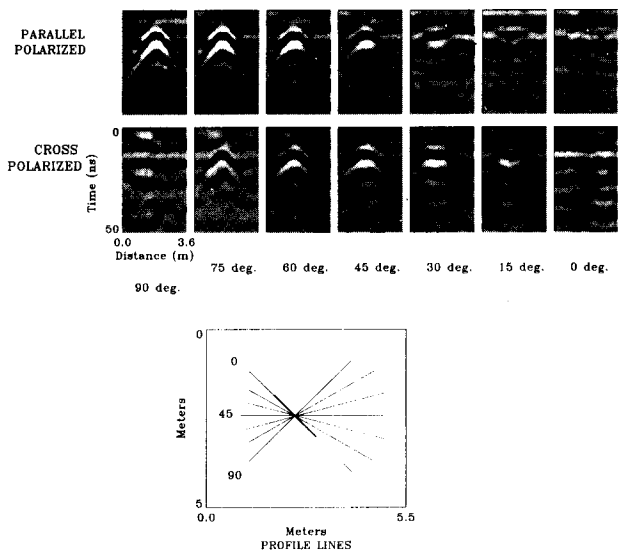

Fig. 11. Parallel (top row) and cross-polarization (bottom row) data from profile lines at different azimuths relative to the long axis of a buried pipe.

0 or 90 degrees relative to the long axis of the pipe. The maximum cross-polarized reflection strength occurs when the profile line crosses the buried pipe at a 45 degree angle.

Combined cross and parallel polarized GPR data interpretation can be useful for target detection and characterization. Research conducted at The Ohio State University ElectroScience Laboratory indicates that by utilizing multiple polarization data collected on a 2-D grid over metallic buried targets, the target's dimensions, depth, and geometry in terms of curved or flat surface are ascertainable.

System Performance and Interpretation

The three field measures of the performance of a GPR system are its depth of penetration, its ability to detect a buried object, and its ability to resolve, or define, the details of a buried object. The depth of penetration of a radar wave depends upon the electrical properties, center band frequency of the antenna, and the power output of the antenna. Dry homogenous rocks and soils (e.g. beach sand, non-vuggy limestone, granite, etc.) can yield penetration depths up to 35 m. However, even in the best of conditions the maximum depth of penetration is usually not more than 10-15 m with an antenna whose frequency is greater than 75 Mhz. Maximum penetration in a soil that is predominantly montmorillonite clay can be as low as a few inches. However, the normal penetration depth for most soils is on the order of a few feet. Lower frequency antennas generally improve the depth of penetration for most soil and rock types. A high frequency antenna (500 Mhz) would provide a detailed image of very shallow features, but it would not penetrate very deeply. A low frequency antenna (50 Mhz) would significantly improve the depth of penetration of the radar wave, but the resolution of very shallow features, would be less distinct.

The resolution and detection capabilities for a system to a specific object depend upon the electrical properties (conductivity and dielectric constant) of the object and the propagation and attenuation characteristics of the

surrounding medium, the geologic and man-made noise that can interfere with the system, the characteristics of the transmitter and receiver, and the reduction, enhancement and display of the data.

Horizontal resolution is the ability of a system to distinguish two objects that are side-by-side. Vertical Resolution is often defined as the ability to distinguish independent reflections from both the top and bottom of an object (e.g. a thin layer) that has different electrical properties than the overlaying, and underlaying medium. If the layer is very thin (in the vertical direction), then the reflection from the top of the layer can interfere with the reflection from the bottom of the layer, which makes it impossible to resolve the two boundaries. Vertical interference of reflection signals can create traces with a very complex reflection signature. For example, internal reflections within a target often interfere with each other, creating a very complex multiple-legged "reflection" signal. Also, a complex response from a shallow target begets a response from a deeper reflector that is at least as complex as the shallow response. In fact, the interference and signal attenuation caused by a shallow target may totally mask any reflection from a deeper target. Interference effects that mask a target are known as clutter. Clutter cannot be removed from a record, but theoretical models can be used to determine the GPR response for multiple objects.

Antenna ringing is a common form of noise on GPR records that masks true reflection signals. It is caused by the fact that the antenna itself reacts to the electromagnetic wave that it is supposed to detect in much the same manner that a "target" reacts, causing reflections within the antenna itself, and reflections from the ground surface. To avoid strong reflections from the ground surface, and maximize the amount of electromagnetic energy imparted into the subsurface, the electrical impedance (which is determined by the antenna's shape and the adjacent resistive and dielectric material) of the antenna is supposed to match the ground. If there is an impedance mismatch, then the result is antenna ringing. All GPR records exhibit some ringing, and the interpreter must be careful to avoid interpreting the ringing as true reflections, from geologic, or structural, features within the media.

From a practical viewpoint, one of the most difficult tasks in the field is to determine if data are valid, and if reflections can be identified on the record. The easiest way to validate field data is to run a test line over known features (eg. a buried pipe, a culvert, a trench, etc.). If it is not possible to make measurements over known objects, then data validity must be determined qualitatively. The data are general valid and good reflections are being obtained, if there are horizontal variations in the coherent *apparent reflections* (any distinctive event that can be traced from scan-to-scan), and the "apparent reflections" cannot be explained by features on the surface (eg. trees, power lines, fences, railroad tracks, etc.). If there is no character to the apparent reflections, then the validity of the data should be questioned.

We cannot change the intrinsic electrical properties of the rocks, or the noise and clutter conditions that are present, but we can control the source-receiver characteristics and improve the interpretation by proper display and interpretation of the data. However, ultimately physics and instrument engineering reach a limit: there are physical limits on transmitter power and receiver sensitivity, and there are rocks with electrical properties that cannot be penetrated by high frequency electromagnetic waves.

APPLICATIONS

Introduction

GPR has been applied to nearly every type of engineering and geotechnical problem, from locating small voids and reinforcing bar in walls, to determining deep geologic features. The following examples represent three studies from different geologic environments, with distinct engineering objectives. The first study involved the use of GPR to detect and map the presence of underground mine workings at an operating open pit mine. The second study shows how GPR might be used to detect and map fluids in the subsurface. This study also illustrates the effect of seasonal variations on GPR records. The third example illustrates the use of GPR for defining a deep geologic feature, and determining the nature of the weathered zone associated with intersecting shear zones.

Example 1: Detecting Underground Voids

Finding an underground opening is one of the most challenging exploration targets for a geophysicist. They occur in a variety of geologic environments, they may be naturally occurring, or man made, they may be deep, or shallow. All of these variables change the physical properties that affect the choice of exploration methods and models that are available to the geophysicists. GPR is an excellent technique for detecting shallow voids (air-filled, or water-filled) since there is always a high contrast in the electromagnetic wave velocity at the boundary between the rock and the cavity.

Individual horizontal and vertical subsurface features have been identified and interpreted to depths exceeding 10 m using GPR data at a mine in Zortman, Montana (Daniels and others, 1992b). The syenite porphyry at the Zortman Mine is homogenous in its electrical properties except where fracturing, faulting or sulfide intrusions occur. Fracturing from drilling and blasting operations is generally confined to the region from the surface down to 1-2 meters below the surface. The examples in Figure 12 illustrate GPR anomalies caused by near-surface fractures in the upper 3 meters (0-45 ns) for Figure 12-a and the upper 1 meter for Figure 12-b (0-to 16 ns) .

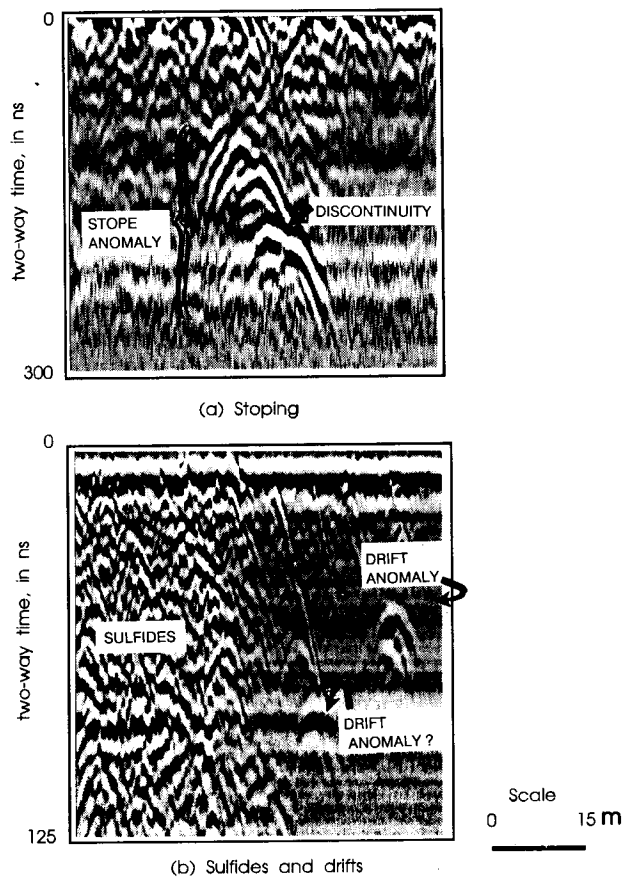

Fig. 12. Examples of GPR anomalies associated with (a) stoping, and (b) sulfides and drifts (from Daniels and others, 1992).

GPR anomalies at the Zortman Mine are generally caused by sulfides, drifts, and vertical features (winzes, manways, and stopes). A typical stope anomaly is shown in Figure 12-a., while anomalies caused by mineralogic sulfides and mine drifts are shown in Figure 12-b. Sulfides generally cause numerous overlapping anomalies, and they often appear as dipping planes

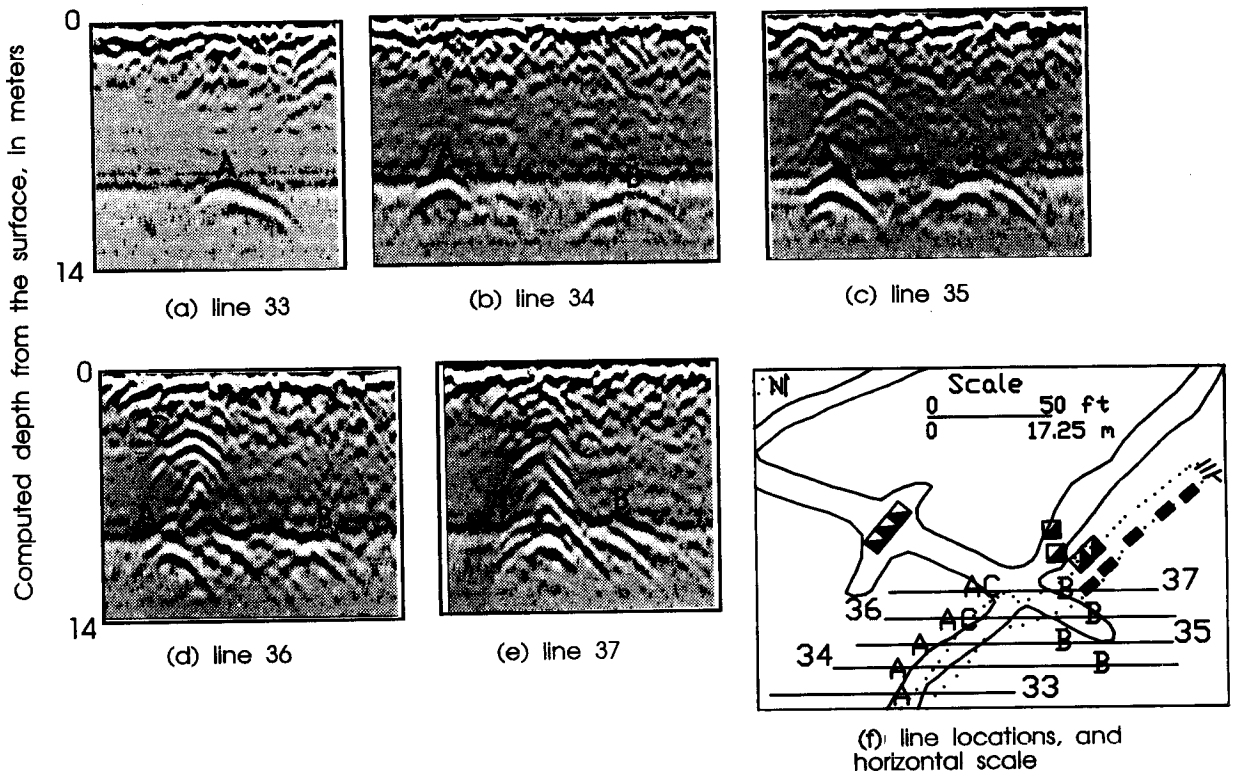

Fig. 13. Sections of GPR lines 33, 34, 35, 36, and 37 across mine workings shown in (f). Horizontal scale of the records is the same as in the index map. Vertical scale is from 0 to 300 ns, or 0 to 14 m, assuming a velocity of 16.4 ns/m (from Daniels and others, 1992).

when they are associated with veins. The anomaly pattern on the left side of Figure 12-b is typical for Zortman sulfide zones. The right side of this zone appears to have an associated fracture that is interpreted as being filled with sulfides causing an anomaly that has characteristics similar to a dipping plane as described by Ulriksen (1982). Anomalies caused by drifts (a horizontal passage way) are usually isolated singular anomalies as shown in Figure 12(b).

Anomalies caused by stopes (a large mined-out region within a drift) are usually complex, containing multiple hyperbolas at different two-way travel times. Open stopes generally yield a very broad, distinct, high-amplitude anomaly that is normally easy to distinguish from a sulfide zone, or a naturally occurring fracture. The lateral discontinuity in the parabola indicated in Figure 12-a is common to many vertical features at Zortman. These abrupt lateral changes in the parabolas are thought to be caused by interference between reflections on different boundaries in the vertical structure. The amount of interference is a function of the size and orientation of the features, with the most interference occurring in nearly vertical winzes, or raises that connect the different mining levels (see Figure 13-e). Vertical fractures are generally present above the stoped regions. These fracture systems cause additional anomalies on the GPR records, and these anomalies indicate that many of the fractures are associated with stoping extent from the stoped depth to the surface of a level.

Parallel GPR profile lines at Zortman were spaced 3.1 m apart. Measurements were made along orthogonal lines when the subsurface workings are oriented in several different azimuthal directions. The GPR records of five parallel lines crossing a major vertical feature are shown in Figure 13.

Figure 14 illustrates GPR anomalies on perpendicular lines crossing over a stope. Anomaly F shown on Line 115 is at the same location as anomaly F on Line 42. Anomaly G on Line 115 is more difficult to distinguish on the east-west lines, but it appears to correlate with the faint anomaly marked D on Line 38. The low intensity and asymmetry of the anomaly is characteristic of anomalies caused by objects that are offset from the primary direction of the line. The interpretation of GPR data for orthogonal lines is clearer for Line 145. Line 145 crosses Line 39 at approximately the location of anomaly A. The general character, size, and intensity of the corresponding anomalies on Lines 145 and 39 are very similar, indicating that the stoping (or caving) causing the anomalies on both lines, is a broad feature extending equally in the north-south and east-west directions.

Since mining operations strip off 6.1 meters of rock at each level, the Zortman data set offers the rare opportunity to compare GPR data from different vertical levels. Corresponding adjacent lines for two different vertical levels are shown in Figure 15. It should be noted that the vertical scales are different on the two data sets. The GPR records in Figure 15 show a general correlation between the anomalies on the vertically coincident lines. The correspondence between anomalies at the two Levels for Lines 36 and 37 is more difficult to establish than for the anomalies on Lines 34 and 35. There are two probable reasons for the increased complexity and poorer correspondence between features on Lines 36 and 37: 1) the vertical raise, that is clearly shown for data at the 4800 Level, causes an increasingly complicated reflection pattern as the raise is penetrated by the mining operations, and 2) the reflection patterns can become very complex for the shallow stoped regions. A GPR cross section is a time-space record of the sum of the reflections and diffractions from the boundaries between contrasts in electrical properties. If the shape of these boundaries is very complex, then the resulting GPR interference patterns are very complex and specific features are difficult to interpret. Furthermore, the apparent complexity of a GPR record increases as the distance from the object decreases, since the

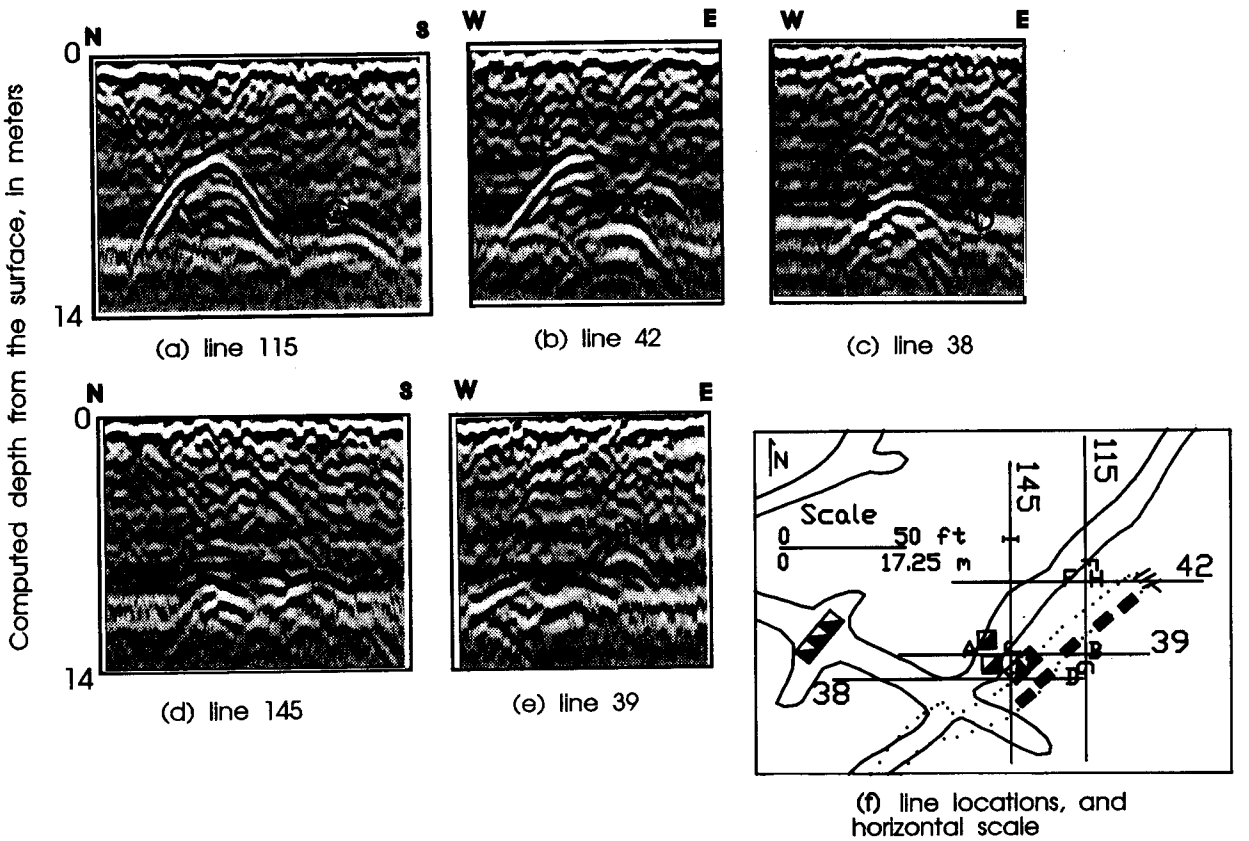

Fig. 14. Sections of GPR north-south lines (a) 115, and (d) 145 crossing east-west lines (b) 32, (c) 37, and (e) 39. Horizontal scale on the records is the same as the index map scale (f). Total vertical scale is 300 ns (from Daniels and others, 1992).

resolution of individual features also increases as the distance decreases.

Example 2: Detecting Subsurface Fluids

The relative electric permittivity of fluids range from approximately 2-30 for hydrocarbon products, to 80 for water. The conductivities of fluids also cover a broad range, from over a 1000 S/m for a conductive brine, to less than 0.01 S/m for many hydrocarbon products. This broad range of electrical properties of fluids makes electrical methods a natural tool for detecting and mapping fluids in the subsurface, with low frequency techniques particularly applicable to locating high conductivity fluids, while high frequency techniques (ground penetrating radar, or GPR) are better suited for detecting contrasts in dielectric constant.

The electrical response of aqueous fluids and the detection of soil moisture have been discussed by Ulriksen (1982), Benson and others, (1984), and other investigators. Very few detailed studies have been conducted on the detectability of non-aqueous phase fluids with high frequency electromagnetic techniques (Olhoeft, 1986; Daniels and others, 1992a). An excellent summary of electrical properties of toxic substances has been provided by Lucius and others (1992).

Hydrocarbon products can be present as light non-aqueous phase liquids (LNAPL's) in the vadose zone and the transition zone (capillary fringe) above the water table, and below the water table as dense non-aqueous phase liquids (DNAPL's). For hydrocarbons, detectability has been assumed to be primarily a function of the relative electric permittivity of the material (e_r). A detectable contrast between the fluid and the host material depends upon the relative contrasts between the different solid and liquid components. The contrast between a hydrocarbon and air, or water, is usually greater than 2:1. Laboratory measurements of e_r for some of the more common hydrocarbons are shown in Table 1. These values indicate a generally low value for LNAPL's, which should not provide a very high contrast with most clean sands and gravel, but the electrical permittivities should have a good contrast with clay soils and loam.

Hydrocarbon products can be present as light non-aqueous phase liquids (LNAPL's) in the vadose zone and the transition zone (capillary fringe) above the water table, and below the water table as dense non-aqueous phase liquids (DNAPL's). For hydrocarbons, detectability has been assumed to be primarily a function of the relative electric permittivity of the material (e_r). A detectable contrast between the fluid and the host material depends upon the relative contrasts between the different solid and liquid components. The contrast between a hydrocarbon and air, or water, is usually greater than 2:1. Laboratory measurements of e_r for some of the more common hydrocarbons are shown in Table 1. These values indicate a generally low value for LNAPL's, which should not provide a very high contrast with most clean sands and gravel, but the electrical permittivities should have a good contrast with clay soils and loam.

Figure 16 illustrates the different phases of a hydrocarbon spill (LNAPL), including: 1) gaseous, 2) liquid, and 3) capillary fringe. The important geophysical point from this figure is that a spill does not cause a simple homogenous, isotropic target that simply disperses and floats on the surface of the water table. The capillary fringe and gaseous phases are strongly affected by the hydrogeology in the vadose zone above the water table.

A study was conducted at a gasoline tank farm in Northern Indiana to

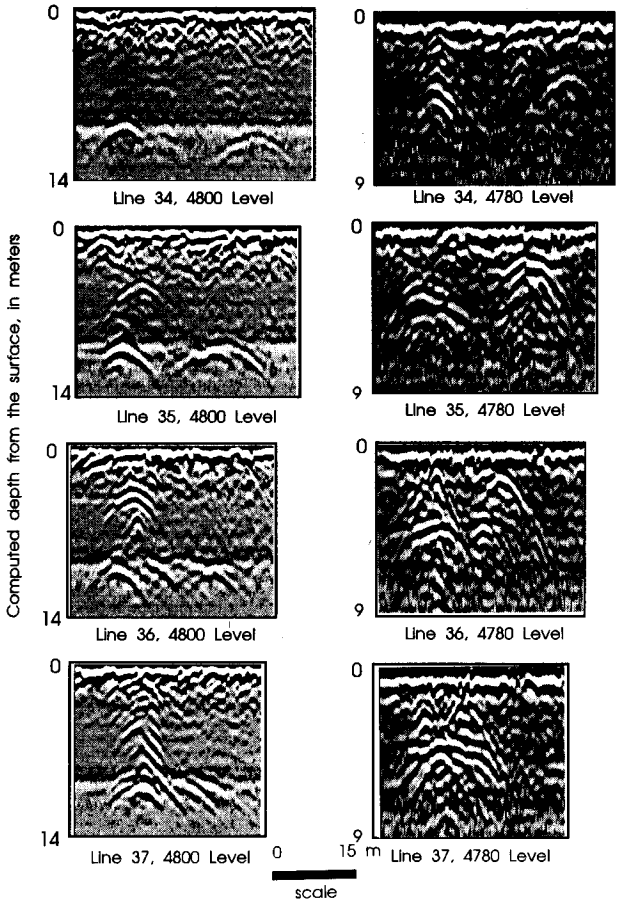

Fig. 15. Comparison of GPR data for coincident lines at two different mining levels (from Daniels and others, 1992).

Table 1. Relative electric permittivities for a few common hydrocarbons (von Hippel, 1961)

Organic Liquid	$1x10^6$	$1x10^7$	$1x10^8$	$3x10^8$	$3x10^9$ Hertz
Methyl alcohol	31	31	31	30.9	23.9
Ethyl alcohol	24.5	24.1	23.7	22.3	6.5
carbon tetrachloride	2.17	2.17	2.17	2.17	2.17
tetrachloroethylene	2.28	2.28	------	------	2.28
aviation gasoline (91 octane)	-----	-----	------	1.95	1.94
Kerosene	------	------	------	------	2.09

determine the effect of seasonal changes and the presence of hydrocarbons on GPR measurements. The near-surface geology at the site is characterized by unconsolidated sand and gravel, with scattered silt and clay. The deposit extends to depths ranging from 23 to 61 m. The water-table depth at the site varies between 6 and 10 m below the surface, and is primarily a function local topography.

The first problem at the site was to determine the effect of seasonal variations. Repeat measurements were made at this site in October of 1990, December of 1990, January of 1991, and August of 1991 along the same profile lines over the course of the study. GPR profile lines were

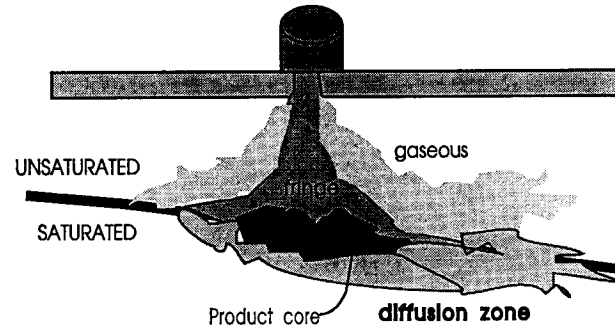

Fig. 16. Subsurface components of a hydrocarbon spill. The capillary fringe, and gaseous zones above the water table. The product core at the water table, and the diffusion zone below the water table (after Schwille, 1967).

concentrated near areas containing hydrocarbons floating on the water table. Water level and hydrocarbon thickness measurements from monitor wells obtained within a day or two of each GPR field excursion show only minor fluctuations in hydrocarbon thickness for the different seasons. The locations of the GPR profile lines at the site are shown in Figure 17. The greatest hydrocarbon thickness at the site was 25 cm, and GPR profile lines C and D crossed a pool of hydrocarbon with a maximum thickness of 15 cm.

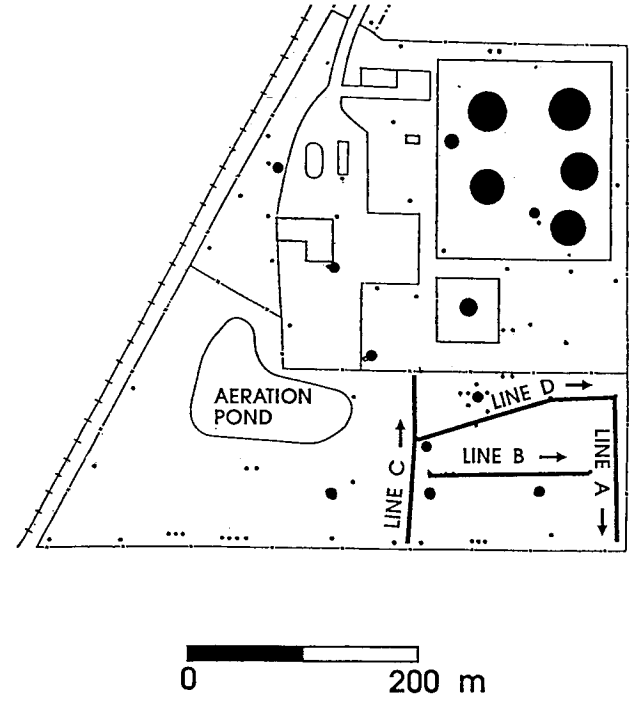

Fig. 17. Study area showing GPR profile lines discussed for the Northern Indiana site.

Each data set was collected in a different climactic setting. Precipitation records from a nearby airport show that the most precipitation fell in October, including 2 cm the day before the October data set was collected.

In August, no precipitation was recorded up to 10 days prior to data collection. The single greatest factor influencing GPR data repeatability was the moisture content in the sandy soil. Line A was located farthest from the contaminant plume. The strong, nearly continuous reflection in each profile line in Figures 18 and 19 is the water table reflection. At first glance, each data set appears unrelated, but closer inspection reveals many correlations between reflections. The December and January data sets are the most similar. There is close agreement between short term rainfall prior to data collection and the similarity of the data sets. The October and August data sets, collected in the wettest and driest conditions, respectively, are the most dissimilar.

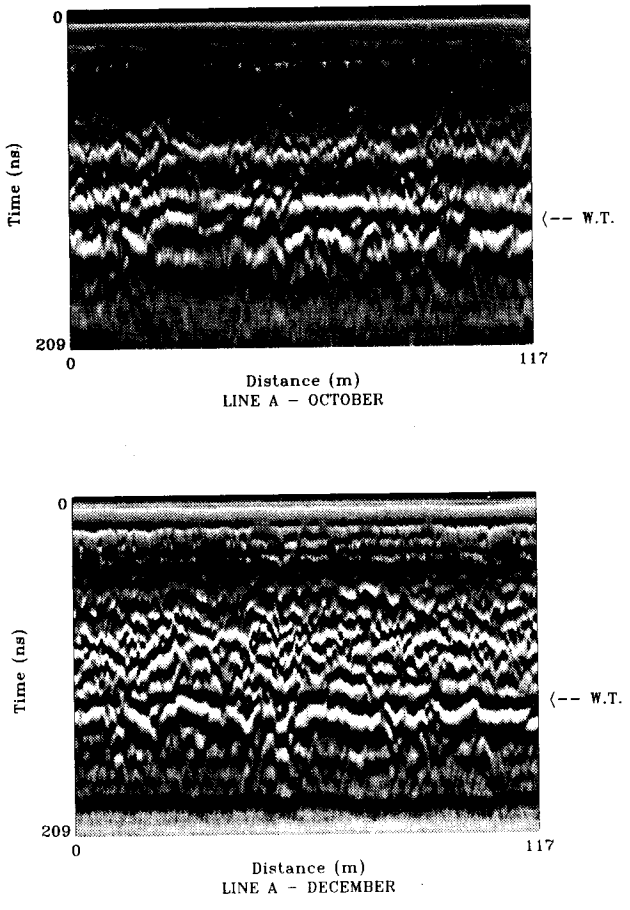

Fig. 18. GPR data from October and December along profile line A.

Hydrocarbon thickness measurements in monitoring wells at the site constrained the GPR interpretation. Portions of profile lines C and D crossed over a hydrocarbon pool with thickness ranging up to 15 cm. The portions of the profile lines crossing over the hydrocarbon consistently have a weakened or non-existent water table reflection. The August data set delineates hydrocarbon presence the best probably because there are no patches of percolating water in the unsaturated zone.

There are inconsistencies in the water table reflections along profile line C (see Figure 20). In the January data set there is a significant water table reflection near the end of line C which is not apparent in the other data sets. The transient appearance of the reflector suggest that the hydrocarbon pools are not continuous, but rather occur as patches. It is also possible that a hydrocarbon patch near the end of line C was migrating, but this is difficult to establish since monitoring wells only sample the hydrocarbon at discrete points.

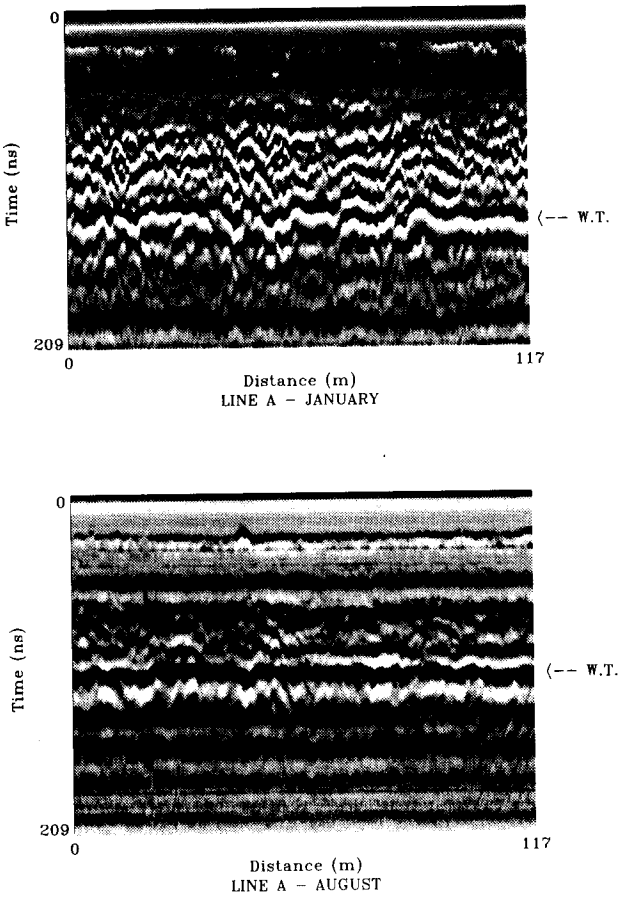

Fig. 19. GPR data from January and August along profile line A.

The correlation between the decreased signal amplitude and the presence of hydrocarbons is illustrated by the records shown in Figure 20. The control line (Line A, Figures 18 and 19) is removed from the concentration of the gasoline, while Line C (Figure 20) extends into the maximum concentration of the gasoline above the water table. The exact reason for the decrease in the received signal amplitude in the vicinity of hydrocarbons is unknown, but there appear to be at least two plausible explanations: 1) scattering losses caused by small dispersed concentrations of hydrocarbons in the capillary fringe, or 2) a very high value for the loss tangent of the hydrocarbon product. There are very few published values for the loss tangent of hydrocarbons in the GPR frequency range. Von Hipple (1961) does provide values for kerosene (45 at 3 x 10^9 Hz), and aviation gasoline (0.4 and 11.5, at frequencies of 3 x 10^8 and 3 x 10^9 hz, respectively). If high loss tangent values are associated with hydrocarbons for frequencies less than 10^9 hz, then it follows that low amplitudes on the GPR records may be caused by hydrocarbon products with the high loss tangent values.

Another observation that can be drawn from Figure 20 is the fact that the amplitude decrease on the GPR record occurs above the water table. The presence of the anomalous response above the water table may be interpreted to be caused by the influence of the vapor phase of the gasoline above the water table. An alternative interpretation is that the decreased amplitude is caused by scattering loss associated with dispersed concentrations of hydrocarbon product in the vadose zone.

Example 3: Defining Shear Zones

Defining the host geology and mapping subsurface faults and other heterogeneities is one of the most important geotechnical applications of the

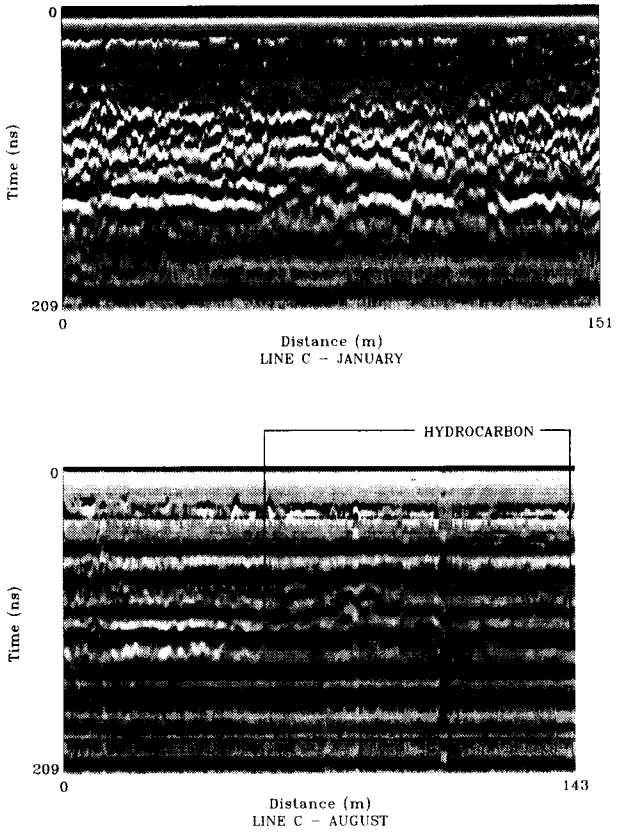

Fig. 20. GPR data from January and August along profile line D.

GPR method. This fact is illustrated for a proposed dam spillway site. The proposed location of the spillway at the Tehri Dam Site in Northern India is situated nearly at the projected intersection of two shear zones that outcrop on the surface. Roughly, the site engineering stratigraphy consisted of 1) an unconsolidated overburden, overlaying 2) a weathered zone, that overlaid the phillitic quartzite basement rock. The original spillway design placed the spillway on top of the basement rock. This design requires the removal of the overburden. Site geologists estimated that the depth of overburden was approximately 15 meters, based on their interpretation of the outcrops. However, excavations at the site indicated that the overburden thickness was greater than 15 meters.

The Central Soil and Material Research Station (CSMRS) in New Delhi, India was requested by Tehri Hydro Development Corp. Ltd. to test GPR at the spillway site to determine if the shear zones could be mapped by the GPR method. Several GPR lines were run across the projected intersection of the two shear zones, which outcropped at the surface to locate these two shear zones, using an 80 Mhz antenna.

One of the GPR records, with a recording time down to 272 ns, is shown in Figure 21. The GPR record shows the intersection of the two shear zones crossing in the subsurface. The shear zones that are mapped on the surface are indicated by the letters A and B. The intersection of these two shear zones is located at approximately point D, which has a two-way travel time of 200 ns. Assuming a two-way reflection travel time of 16.4 ns/m, then the depth of this intersection point is approximately 12 m. However, it should be noted that the strike directions of the two shear zones are probably not parallel to each other, and the orientation or lines 1 through 8 are not perpendicular to the strike direction of the shear zones. The deep GPR record also shows other interesting features. Letter C on Figure 21 is

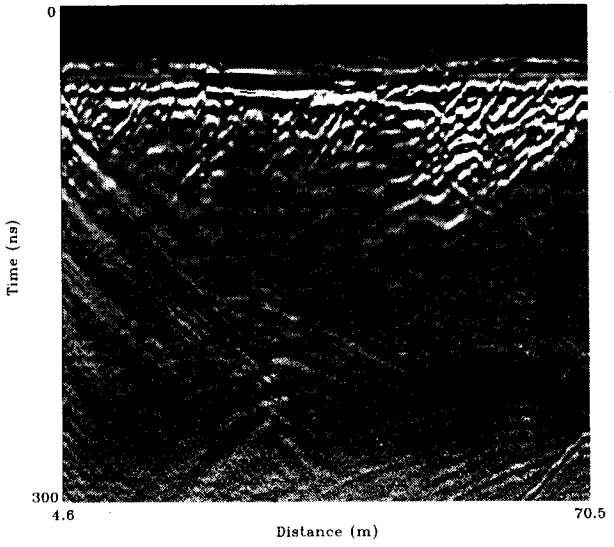

Fig. 21. GPR profile over shear zones, Tehri Dam Site, Northern India. Data courtesy of Central Soil and material Research Station, New Delhi, India).

placed at an anomaly that appears as a drag fold. This may be a compressional feature located at the intersection of the shear zones. Two reflectors located just below letter E indicate that the maximum penetration of the radar is probably much deeper than the 270 ns measured on this record.

The spillway GPR data also show the complexity of the geology at the spillway site. The shear zones do not necessarily mark the boundary between "overburden" and bedrock. Sharp reflections from the "overburden" above the shear zones are parallel to the apparent bedding orientations below the shear zones. This fact implies that the overburden is simply the phyllitic quartzite that has been intensely weathered, with some remanents of the original bedrock remaining intact within the overburden.

CONCLUSIONS

Ground penetrating radar has a great future for geotechnical applications. It has already proven effective for investigating the subsurface in many different situations. It is a method that is relatively easy to use, and can provide a detailed image of the subsurface. There are several limitations of GPR that must be overcome before its potential for subsurface imaging can be fully realized. These problems include: 1) the limited depth of penetration (particularly in clay-rich soils), 2) antenna ringing and other spurious electromagnetic noise that mask targets, 3) the availability of adequate three dimensional data display capabilities, 4) the availability of adequate modeling and target identification capabilities, and 5) the absence of procedures for integrating subsurface geophysical data with existing geotechnical data. It is anticipated that many of these problems will be overcome in the near future, and that GPR will become one of the primary subsurface investigation techniques for geotechnical engineers.

Acknowledgments

The authors would like to thank the continued technical support and positive critical input of Leon Peters Jr., Jonathan Young, and Michael Poirier at The Ohio State University ElectroScience Laboratory. We would also like to thank the scientists at the Central Soil and Material Research Station in New Delhi, India. In addition, we would like to recognize the continued support of the U.S. EPA. In particular, we would like to thank Aldo Mazzella (EMSL, Las Vegas, Nevada) and Mark Vendl (Region V, Chicago, IL).

Notice

Although the research described in this article has been supported by the United States Environmental Protection Agency through Assistance Agreement No. CR-814928 to The Ohio State University Research Foundation, it has not been subjected to Agency review and therefore does not necessarily reflect the views of the Agency and no official endorsement should be inferred. Mention of trade names or commercial products does not constitute encorsement or recommendation for use.

References

Benson, R.C., Glaccum, R. and Noel, N.R., 1984, Geophysical techniques for sensing buried wastes and waste migration, an applications review: in Surface and borehole geophysical methods in ground water investigations, D.M. Nielsen, ed., Natl. Water Well Assoc., Dublin, Ohio, p.533-566.

Daniels, D.J., Gunton, D.J., and Scott, H.F., 1988, Introduction to subsurface radar: IEE Proceedings-F, v. 135, Part F., no. 4, p. 278-320.

Daniels, J.J., 1989, Fundamentals of Ground Penetrating Radar: Proceedings of the Symposium on the Application of Geophysics to Engineering and Environmental Problems, March 13-16, 1989, Society of Mining and Engineering Geophysicists, Denver, CO.

Daniels, J., Roberts, R., and Vendl, M., 1992a Site studies of ground penetrating radar for monitoring petroleum product contaminants: Transactions of the Symposium on the Application of Geophysics to Engineering and Environmental Problems, April 26-29, 1992.

Daniels, J.J., Harris, D., Roberts, R., and Schilling, B., 1992b, GPR measurements for locating underground mine workings at an active open-pit mine, in Fourth International Conference on Ground Penetrating Radar, June 8-13, 1992, Rovaniemi, Finland, Geological Survey of Finland, Special Paper 16, p. 237-246.

Lucius, Jeffrey E., Olhoeft, Gary R., Hill, Patricia L., and Duke, Stephen K., 1992, Properties and hazards of 108 selected substances - 1992 Edition: U.S. Geological Survey Open-File Report 92-527, September 1992, 554 p.

Miller, E.K., 1986, Time-domain Measurements in Electromagnetics: Van Nostrand, New York,536p.

Olhoeft, G.R., 1986, Direct detection of hydrocarbon and organic chemicals with ground penetrating radar and complex resistivity: in Proc. of the NWWA/API Conf. on Petroleum Hydrocarbons and Organic Chemicals in Ground Water -- Prevention, Detection, and Restoration, Nov. 12-14, 1986, Houston: Dublin, Ohio, Nat., Water Well Assoc., p. 284-305.

Roberts, R.L., Daniels, J.J., and Peters, L., 1993, Accounting for near-field conditions when interpreting 3-D GPR data, in Transactions of the Symposium on the Application of Geophysics to Engineering and Environmental Problems: Environmental and Engineerign Geophysical Society, San Diego, April 18-22, 1993.

Ulriksen, C Peter F, 1982, Application of impulse radar to civil engineering: Doctoral Thesis, Department of Engineering Geology, Lund University of Technology, Lund, Sweden, reprinted and distributed by Geophysical Survey Systems Inc., Hudson, NH, USA.

Von Hippel, A.R., (editor), 1961, Dielectric materials and applications: The M.I.T. Press, Cambridge, Mass., 438 p.